Conductivity-modulus-Tg relationships in solvent-free, single lithium ion conducting network electrolytes

Chengtian Shen^{1,3}, Qiujie Zhao^{2,3}, Naisong Shan^{1,2,3}, Brian B. Jing^{2,3,4} and Christopher M. Evans^{2,3,4}

³Frederick Seitz Materials Research Laboratory, University of Illinois at Urbana-Champaign, Urbana, IL, 61801, USA

⁴Beckman Institute for Advanced Science and Technology, University of Illinois at Urbana-Champaign, Urbana, IL, 61801, USA

Correspondence Christopher M. Evans, Department of Materials Science and Engineering, University of Illinois at Urbana-Champaign. 202A Materials Science & Engineering Building, 1304 W. Green,

Urbana, Illinois.

Email: cme365@illinois.edu

ABSTRACT

A model system of single ion conducting network electrolytes with acrylic backbone, ethylene oxide (EO) side chains, tethered fluorinated anions, and mobile Li cations was designed and synthesized to investigate structure-property relationships. By systematically tuning four molecular variables, one at a time, we investigated how crosslinker length, mol% of crosslinker added, Li:EO ratio and side chain length affect conductivity, T_g and modulus. Ionic conductivity at 90 °C varied by two orders of magnitude (and by three orders of magnitude at room temperature) depending on the molecular details, while a 70 °C span in glass transition temperature (T_g) was observed. The range of crosslinking which can be achieved without impacting conductivity was also elucidated, and the modulus of the electrolyte can be increased by a factor of 8, up to 2.4 MPa, without impacting ion transport. Changes in conductivity due to crosslink density and crosslinker length are fully explained in terms of T_g shifts, while comonomer length cannot be accounted for by such a shift. The best performing network exhibited 10^{-5} S/cm at high temperature, which is comparable to other single ion conductors reported in the literature, while the modulus is higher

¹Department of Chemistry, University of Illinois at Urbana-Champaign, Urbana, IL, 61801, USA ²Department of Materials Science and Engineering, University of Illinois at Urbana-Champaign, Urbana, IL, 61801, USA

due to crosslinking. Adding 10 wt.% propylene carbonate further increased this value to 10⁻⁴ S/cm. This work provides insights on structure-property relationships of solid-state polymer electrolytes which retain conductivity but can potentially help suppress dendrites.

Key words: Li⁺ single ion conductors, crosslinked ionic polymers, solid state polymer electrolytes, Li battery electrolytes, structure-property relationship

1. INTRODUCTION

As recognized by the 2019 Noble Prize, Li-ion batteries are an important part of our current and future energy storage strategies. Despite a high theoretical specific capacity (3860 mAh/g), ¹⁻³ the growth of metallic dendrites during prolonged cycling can lead to shorting, overheating, and ignition of organic liquid electrolytes. ⁴⁻⁸ Safety concerns have hindered the broad application of such batteries and motivated the development of solid polymer electrolytes (SPE) which are in principle safer and less flammable, albeit with typically much lower ionic conductivities. Despite many publications on new SPEs, structure-property relationships are still being investigated to understand how mechanical properties and conductivity (σ) are impacted by polarity, the glass transition temperature (Tg), crystallinity, alignment, and architecture.

Polymers networks containing ionic species have received attention as functional materials in liquid/gas separations, ⁹⁻¹⁵ soft actuators, ¹⁶⁻²⁰ ion exchange membranes, ²¹⁻²⁵ and electrolytes for energy storage. ²⁶⁻³⁵ In the context of lithium conduction, polyethylene oxide (PEO) networks with added lithium salts have been investigated and it was shown that covalent crosslinking can significantly reduce the crystallinity and increase the ionic conductivity. ³⁶⁻³⁸ Dual ion conducting electrolytes based on acrylates, ²⁷ polyethylene, ²⁸ polyacrylonitrile, ³⁹ epoxy, ⁴⁰ and PEO networks ⁴¹⁻⁴³ with Li salts have also been investigated and often show dendrite suppression capabilities when cycled with a Li electrode. These systems are effective presumably because the network must

break for propagation of the dendrite front, ^{27-28, 31, 39-42} and even relatively soft (~10⁵ Pa) electrolytes are capable of dendrite suppression. In dual ion conductors, the transference number of lithium (t_{Li}^+) is usually less than 0.5, although the measurement and interpretation of these values are still the subjects of much discussion.^{3,44-47} According to the simulation work by Monroe and Newman⁴⁸, Li dendrites will not form when t_{Li}^+ is equal to 1 due to the absence of concentration gradients in the system and in particular at the dendrite front.^{3,7} High transference numbers are pursued by fixing the anions onto the polymer matrix, forming a single ion conductor. Such single ion conducting gel systems (filled with electrochemically stable organic solvent) have t_{Li} higher than 0.5 and they have shown better dendrite suppression capability. ^{29, 49-51} Most commonly, a derivative of trifluoromethane sulfonimide is tethered to a linear, random, or block copolymer, 51-54 or a network. 29, 49-50, 55 The advantages of a network structure and improved transference number make crosslinked Li⁺ single ion conductors an attractive candidate for safer solid state electrolyte with improved dendrite suppression capability. Although block copolymers can have higher modulus, 53-54, 56 they also present tortuous pathways for ions and alignment may be important for efficient conduction. To our knowledge, there is only one report of network Li⁺ single ion conductors without added solvent⁵⁵ and there is still much unknown about basic structure-property relationships.

A general tradeoff between ionic conductivity and mechanical strength is observed in linear single ion conductors or polymerized ionic liquids (PILs). High T_g PILs have greater mechanical stability but lower ionic conductivity due to lower segmental mobility.⁵⁷ Many groups have noted the important roles of polarity, ion concentration, polymer morphology and segmental dynamics on conductivity in linear single ion conducting systems.^{21, 57-60}. Prior works on single anion conducting network polymers have investigated the roles of network versus linear architecture,³⁵

precise length of carbon spacers between network junctions,⁶¹ crosslinking density,^{16, 62-63} ionic interactions,^{55, 63-64} and ion concentration⁵⁵ on ion transport through changes in T_g and mechanical properties. However, there is still a need for systematic studies of Li⁺ single ion conducting networks with controlled architecture, charge density, and mechanical properties to understand how performance is related to molecular structure. Studies without added solvent are necessary to focus specifically on the role of the polymer chemistry and architecture.

A model single ion conducting polymer network platform was designed such that systematic control of the mole percent of crosslinker (from 1-50 mol%), the length of the crosslinker (11, 17, or 35 atoms), the lithium to ethylene oxide (Li:EO) ratio (1:20 to 1:100), and the length of the side chain (11 or 19 atoms) was achieved. Changes in these molecular parameters elicit a three orders of magnitude difference in ionic conductivity (at room temperature, solvent free) and a 70 °C shift in T_g. In lightly crosslinked networks, the modulus of the electrolyte can be increased by a factor of 8 without sacrificing conductivity. A T_g-normalization of conductivity can account for changes in percent of crosslinker and the length of the crosslinker but cannot account for changes in the side chain length or Li:EO ratio. The observed structure-conductivity trends provide insight into the rational design of single ion conductors for a broad range of energy applications.

2. EXPERIMENTAL SECTION

Oxalyl chloride (\geq 99%), *N,N*-dimethylformamide (DMF, anhydrous, 99.8%), 3-sulfopropyl acrylate potassium salt, sodium bicarbonate (\geq 99.7%), 3-sulfopropyl methacrylate potassium salt (98%) sodium chloride (\geq 99%), magnesium sulfate (\geq 99.5%), potassium carbonate (99.99%), dimethyl sulfoxide (anhydrous, \geq 99%), acryloyl chloride (\geq 97%), methacryloyl chloride (97%, 200 ppm monomethyl ether hydroquinone as stabilizer), butylated hydroxytoluene (BHT, \geq 99%), lithium perchlorate (\geq 99.99%), tetraethylene glycol (\geq 99%), 2,2° azobis(2-methylpropionitrile)

(AIBN, 98%) were purchased from Sigma Aldrich and used as received. Dichloromethane (DCM, HPLC), acetonitrile (MeCN, anhydrous, 99.8%), triethylamine (TEA, ≥99.7%) were purchased from Sigma Aldrich and stored with activated molecular sieves to remove water. Trifluoromethanesulfonamide (>98%), hexaethylene glycol monomethyl ether (>96%), triethylene glycol monomethyl ether (>98%) were purchased from Tokyo Chemical Industry Co., LTD (TCI) and used without further purification. Dodecaethylene glycol (≥95%) was purchased from JenKum Technology and used as received. Hexaethylene glycol (≥96%) was purchased from Alfa Aesar and used without purification. Hexanes (Hex, ≥98.5%, with 4.2% methylpentanes), Ethyl acetate (EtOAc, ≥99.5%), Methanol (MeOH, HPLC grade) were purchased from Fischer Chemical and used as received.

2.1. Synthesis of monomers and crosslinkers

2.1.1. Synthesis of the ionic monomer

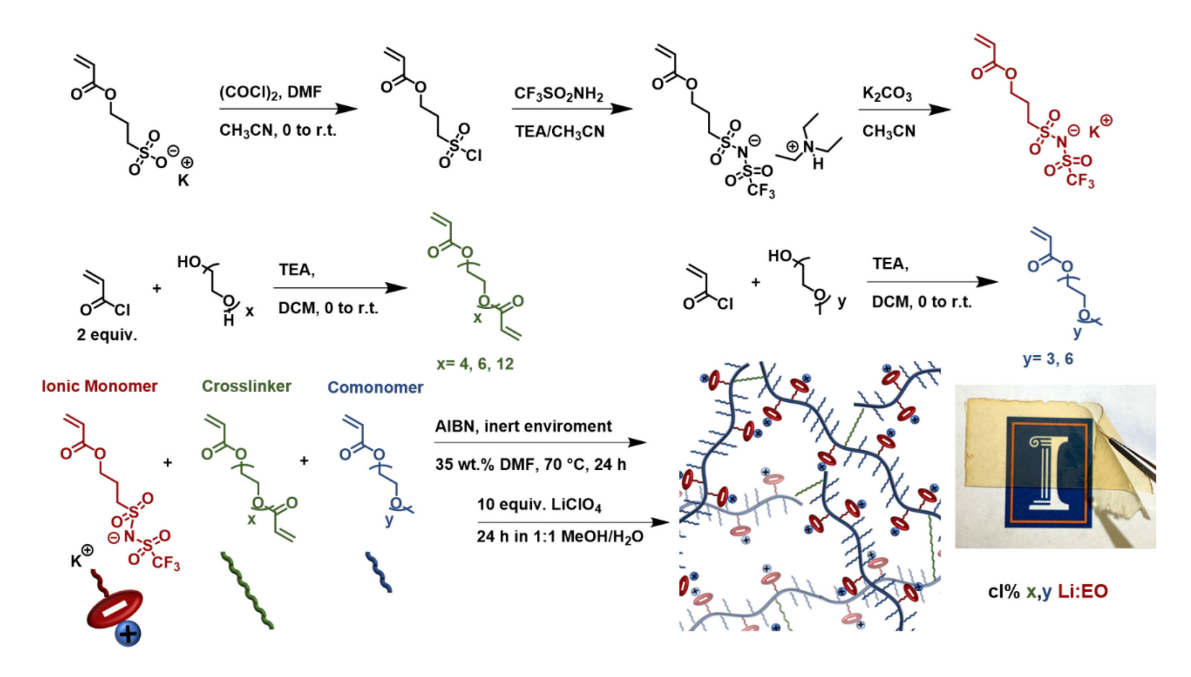


Figure 1. Synthesis of monomers for crosslinked Li^+ conducting electrolytes. An ionic monomer, crosslinker, and commoner were polymerized and are named based on the mole percent of crosslinker added (cl%), the crosslinker length (x), comonomer side chain length (y), and salt content in terms of Li:EO ratio. A photo shows the general appearance of the electrolytes.

The synthesis of 3-sulfonyl(trifluoromethane sulfonyl) imide propyl acrylate ionic monomer was performed following a literature procedure⁶⁵ with a minor modification in purification conditions (Figure 1). In a 300 mL, oven dried round bottom flask a solution of DMF (1.5 mL, 19.4 mmol) in anhydrous MeCN (90 mL) was cooled to 0 °C under N2 atmosphere. Oxalyl chloride (7.2 mL, 84.2 mmol) was added into the reaction flask drop-wise as gas bubbles exited from the reaction mixture. The mixture was then stirred for 1 hr at room temperature while white precipitates formed. Potassium 3-sulfopropyl acrylate (15.05 g, 64.8 mmol) was then added into the reaction flask under a positive pressure of N₂ at 0 °C. With the evolution of HCl gas, the mixture was stirred for 3 hrs at 0 °C and 2 hrs at room temperature to form 3-(chlorosulfonyl) propyl acrylate. In a separate dry round bottom flask, a solution of trifluoromethanesulfonamide (8.00 g, 53.7 mmol) and anhydrous triethylamine (20.2 mL, 145.0 mmol) in 30 mL anhydrous MeCN was well mixed and transferred to the 3-(chlorosulfonyl) propyl acrylate reaction flask via cannula while both mixtures were cooled to 0 °C under N₂. The reaction mixture was allowed to reach room temperature and stirred for an additional 18 hrs. Vacuum filtration was used to remove salts from the reaction after completion, and MeCN was removed using rotary evaporation. The remaining crude mixture was dissolved into DCM and washed with a saturated NaHCO₃ solution, 1 M HCl and brine. The organic phase was dried over MgSO₄ and concentrated to afford a brown oil. Product was confirmed by ¹H NMR. The resulting ammonium ionic monomer from the previous step (64.8 mmol) was dissolved into 200 mL MeCN followed by the addition of K2CO3 (17.9 g, 129.6 mmol). The reaction was allowed to stir at room temperature for 5 hrs. The excess K₂CO₃ was filtered off via vacuum filtration and the filtrate was collected and concentrated to obtain a brown solid. Recrystallization of the crude product was done in MeCN and yielded a white/light brownish powder. ¹H NMR (500 MHz, DMSO-d₆) δ (ppm): 6.33 (d, 1H, -CH₂=CH₂-), 6.18 (dd, 1H, -CH₂=CH₂-), 5.93 (d, 1H, -CH₂=CH₂-), 3.05 (t, 2H, -CH₂CH₂-O-), 2.01 (q, 2H,-CH₂CH₂-O-). ¹³C NMR (500 MHz, DMSO-d₆) δ (ppm): 165.84, 132.02, 128.71, 70.23 (q, CF₃), 63.02, 51.71, 23.98.

Synthesis of a methyl methacrylate (MMA) version of the ionic monomer followed the above procedure with 3-sulfopropyl methacrylate potassium salt as the starting material. The final product was a white powder (35 % yield). ¹H NMR (500 MHz, DMSO-d₆) δ (ppm): 6.04 (s, CH₂=C, 1H), 5.67 (s, CH₂=C, 1H), 4.17 (t. CH₂-O, 2H), 3.06 (quint, CH₂-S, 2H), 2.00 (t, C-CH₂-C, 2H), 1.87 (s, C-CH₃, 3H). ¹³C NMR (500 MHz, DMSO-d₆) δ (ppm): 165.63, 131.82, 130.84, 129.66, 128.38, 69.93, 69.90, 68.38, 63.62.

2.1.2. Synthesis of EO crosslinkers with x = 4, 6, 12

As shown in Figure 1, an EO12 crosslinker was formed starting with dodecaethylene glycol (1.05g, 5.39 mmol) deoxygenated under nitrogen in a round bottom flask. Anhydrous triethylamine (1.309g, 12.94 mmol) and anhydrous DCM (18 mL) were added to the flask. Acryloyl chloride (1.17g, 12.94 mmol) was added dropwise to the flask with constant stirring at 0 °C. The reaction proceeded 18 hrs at room temperature and the completion was confirmed by TLC. After that, DCM and excess acryloyl chloride were evaporated and the crude product was purified by column chromatography (5% MeOH in EtOAc, $R_f = 0.3$). 200 ppm butylated hydroxytoluene (BHT) was added before vacuum drying at room temperature overnight. The final product is a colorless oil. 1 H NMR (500 MHz, CDCl₃) δ (ppm): 6.32 (d, 2H, -CH₂=CH₂-), 6.18 (dd, 2H, -CH₂=CH₂-), 5.93 (d, 2H, -CH₂=CH₂-), 4.22 (t, 4H, -CH₂CH₂-O-), 3.62 (m, 4H, -CH₂CH₂-O-), 3.48 (m, 40H, -CH₂CH₂-O-). 13 C NMR (500 MHz, DMSO-d₆) δ (ppm): 165.92, 132.13, 128.67, 70.24, 68.69, 63.93.

The EO6 and EO4 crosslinkers followed the same synthetic procedure with different starting

materials (hexamethylene glycol and tetraethylene glycol) and column condition: EO4 (20% Hex in EtOAc), EO6 (100% EtOAc). The EO6 crosslinker is a colorless oil. ¹H NMR (500 MHz, CDCl₃) δ (ppm): 6.43 (d, 2H, -CH₂=CH₂-), 6.19 (dd, 2H, -CH₂=CH₂-), 5.95 (d, 2H,-CH₂=CH₂-), 4.32 (t, 4H, -CH₂CH₂-O-), 3.7 (m, 20H, -CH₂CH₂-O-). ¹³C NMR (500 MHz, DMSO-d₆) δ (ppm): 165.92, 132.13, 128.68, 70.24, 68.69, 63.93, 60.22 21.22, 14.55. The EO4 crosslinker is a colorless oil. ¹H NMR (500 MHz, DMSO-d₆) δ (ppm): 6.34 (d, 2H, -CH₂=CH₂-), 6.20 (dd, 2H, -CH₂=CH₂-), 5.96 (d, 2H, -CH₂=CH₂-), 4.22 (t, 4H, -CH₂CH₂-O-), 3.65 (m, 4H, -CH₂CH₂-O-), 3.53 (m, 8H, -CH₂CH₂-O-). ¹³C NMR (500 MHz, DMSO-d₆) δ (ppm): 165.92, 132.12, 128.67, 70.23, 70.21, 68.69, 63.92.

The MMA version of EO12 crosslinker was synthesized using the above procedure but with methacryloyl chloride as the reactant. The crude product was purified with flash column chromatography (5% MeOH in EtOAc, $R_f = 0.1$) to yield a colorless oil. ¹H NMR (500 MHz, CDCl₃) δ (ppm): 6.13 (s, CH2=C, 2H), 5.57 (s, CH2=C, 2H), 4.29 (t, CH2-O, 4H), 3.64 (m, CH₂-CH₂-O, 44H), 1.95 (s, C-CH₃, 6H). ¹³C NMR (500 MHz, DMSO-d₆) δ (ppm): 171.95, 166.99, 136.28, 135.82, 126.29, 103.80, 81.44, 70.32, 70.25, 70.22, 68.72, 68.68, 64.62, 64.21, 30.57, 25.30, 24.66, 18.45, 18.35.

2.1.3. Synthesis of EO comonomers with y = 3, 6

Triethylene glycol monomethyl ether (10.26 g, 61.23 mmol) was deoxygenated under nitrogen in a round bottom flask. Anhydrous triethylamine (15.02 g, 146.95 mmol) and anhydrous DCM (180 mL) were added to the flask. Acryloyl chloride (6.857 g, 73.48 mmol) was added dropwise to the flask with constant stirring. The reaction proceeded 18 hrs at room temperature. Next, DCM and excess acryloyl chloride were evaporated, and the crude product was purified by column chromatography (50% EtOAc in Hex, $R_f = 0.7$). 200 ppm BHT was added before vacuum

drying at room temperature for 24 hrs. The final product is a colorless oil. ¹H NMR (500 MHz, DMSO-d₆) δ (ppm): 6.33 (d,1H,-CH₂=CH₂-), 6.19 (dd,1H,-CH₂=CH₂-), 5.95 (d,1H,-CH₂=CH₂-), 4.22 (t, 2H, -CH₂CH₂-O-), 3.64 (m,2H,-CH₂CH₂-O-), 3.52 (m,6H,-CH₂CH₂-O-), 3.42 (m,2H,-CH₂CH₂-O-), 3.23 (S,3H,-CH₃). ¹³C NMR (500 MHz, DMSO-d₆) δ (ppm): 165.92, 132.13, 128.68, 71.72, 70.25, 70.18, 70.06, 68.69, 63.92 58.51.

Synthesis of EO6 comonomer followed a similar path except hexaethylene glycol monomethyl ether was used. The crude product was purified by column chromatography (100% EtOAc, $R_f = 0.4$) to yield a colorless oil. ¹H NMR (500 MHz, CDCl₃) δ (ppm): 6.43 (d,1H,-CH₂=CH₂-), 6.15 (dd,1H,-CH₂=CH₂-), 5.84 (d, 1H,-CH₂=CH₂-), 4.31 (t, 2H, -CH₂CH₂-O-), 3.74 (M,2H,-CH₂CH₂-O-), 3.65 (M, 18H,-CH₂CH₂-O-), 3.55 (M,2H,-CH₂CH₂-O-), 3.37 (S,3H,-CH₃). ¹³C NMR (500 MHz, DMSO-d₆) δ (ppm): 165.93, 132.14, 128.68, 71.74, 70.26, 70.19, 70.04, 68.69, 63.94, 58.51.

The MMA version of the EO3 comonomer was synthesized following the above procedure with methacryloyl chloride as the reactant. The crude product was purified with flash column chromatography (50% EtOAc in Hex, R_f = 0.1) to yield a colorless oil (28%). ¹H NMR (500 MHz, CDCl₃) δ (ppm): 6.13 (s,CH₂=C, 1H), 5.57 (s,CH₂=C, 1H), 4.29 (t,CH₂-O, 2H), 3.75 (t,CH₂-CH₂-O, 2H), 3.66 (m,CH₂-CH₂-O, 6H), 3.54 (m,CH₂-CH₂-O, 2H), 3.38 (s,O-CH₃, 3H), 1.95 (s,C-CH₃, 3H). ¹³C NMR (500 MHz, DMSO-d₆) δ (ppm): 170.32, 170.30, 166.50, 135.82, 135.36, 125.78, 125.76, 125.75, 124.90, 103.30, 80.96, 71.27, 69.85, 69.73, 69.60, 68.24, 64.12, 63.72, 58.02, 30.95, 30.08, 24.82, 24.16, 22.06, 20.72, 20.70, 17.95, 17.94, 17.84, 14.05.

2.2. Synthesis of crosslinked Li⁺ single ion conducting electrolyte

As one example, to synthesize a 1% 12,6, 1:30 network, EO6 monomer (0.25 g, 0.7135 mmol),

EO12 crosslinker (0.0057 g, 0.0087 mmol), ionic monomer (0.053 g, 0.146 mmol), 2,2' azobis(2-methylpropionitrile) (AIBN, 0.0014 g, 0.0088 mmol) and anhydrous DMF (93 μL) were well mixed in a 5 mL vial. After deoxygenating with nitrogen for 1 hr, the vial was brought into the glovebox. The solution was cast into a custom glass mold which is made of two glass slides, one layer of Kapton spacer (150 μm thick) and vacuum grease as a seal. The glass mold was heated at 70 °C for 24 hrs. The crosslinked network was then carefully peeled off from the mold and submerged into a solution of lithium perchlorate (0.155 g, 1.46 mmol) in 50 mL 1:1 MeOH: H₂O. The ion exchange proceeded two days with constant stirring and fresh salt solution was switched after the first 24 hrs of ion exchange. Next, excess salt solution was removed by washing the network with fresh 1:1 MeOH:H₂O solution. The salt removal was confirmed by measuring the ionic conductivity of the wash solution until it read < 0.5 μS/cm. The network was then vacuum dried at 80 °C for 24 hrs before stored in glovebox for further use. For other samples, the mol% of crosslinker added (cl%), comonomer (co%) and ionic monomer (im%) can be calculated based on following two formulas:

$$im\% + cl\% + co\% = 100\%$$

$$\frac{im\%}{(x-1)cl\% + y * co\%} = \frac{Li}{EO}$$

Where x is the number of EO repeating units of crosslinker, and y is the number of EO repeating units of comonomer. When calculating the total EO units, oxygens from esters are excluded for consistency between the comonomers (y) and crosslinker (x-1). By fixing cl%, the percentages of crosslinker and commoner can be easily calculated to reach a given Li:EO ratio. The synthetic procedure for all networks is identical except the PMMA version of the network uses all MMA type monomers.

2.3. Nuclear magnetic resonance spectroscopy

Solution state 1 H and 13 C NMR was done in the NMR lab of School of Chemical Sciences(SCS) at UIUC with Carver B500, UI500NB or VXR500 (500-MHz) at 23 °C. Solid state 13 C NMR was done in the NMR lab of School of Chemical Sciences at UIUC using Varian Unity Inova instrument (UI300WB, 300 MHz) via direct polarization magic angle spinning (DPMAS) method at 10 kHz spinning frequency with 5600 scans, and 5 s cycle delays ($d_1 = 5$ s). A pseudo T_1 measurement was done with $d_1 = 1$, 5, 10 and 20 s to ensure 5 s is sufficient for all 13 C nuclei to relax.

2.4. Thermal characterization.

Differential scanning calorimetry samples were prepared and sealed with Tzero pans in the glovebox to minimize the influence of moisture. The T_gs of the network were measured using a DSC (Q2500, TA instruments) from -100 °C to 50 °C at a heating/cooling rate of 10 °C/min. The half-point of ΔC_P was used to determine the T_gs of the samples. The thermal stability of each network was measured using a TGA (Q50, TA instruments) from 20 °C to 600 °C at a heating rate of 10 °C/min. The degradation temperature is defined where 5 wt.% of the mass sample is lost.

2.5. Elemental analysis

Inductively coupled plasma mass spectrometry was done by submitting dry samples (packed and sealed in the glovebox) to the SCS Microanalysis Laboratory at UIUC (PerkinElmer Optima 8300). The ratio of Li to K allows us to quantify the ion exchange.

2.6. Mechanical Characterization

Rectangular samples of the networks were loaded onto a Dynamic Mechanical Analyzer (Q800, TA instruments). To remove the water absorbed from air during loading, samples were first heated

to 120 °C and held at 120 °C for 30 mins. Samples were then cooled to room temperature with dry N₂. A controlled force experiment was done with pre-loading force of 0.001 N to obtain a stress vs. strain curve. The Young's modulus of the network samples was reported based on the slope of the linear region of the stress vs. strain curves.

2.7. Electrochemical Characterization

The ionic conductivities of the network electrolytes were measured using electrochemical impedance spectroscopy. A 4 mm diameter circular disk was punched from the synthesized network sheet and placed between two polished stainless-steel electrodes with one layer of Kapton as the spacer. The impedance spectrum was measured using a Biologic SP300 potentiostat at controlled temperature with constant dry N_2 flow in a heating chamber. The thickness was checked before and after the measurement to ensure no significant deformation of the network. The impedance data was processed to make a plot of real (σ ') and imaginary (σ '') conductivities versus frequency. The network ionic conductivity was taken where tan $\delta = \sigma'/\sigma''$ is at a maximum, corresponding to a plateau in the real conductivity.

The Li+ transference number is measured by potentiostatic polarization experiments in CR2032 coin cells assembled with symmetric metallic Li electrodes and a network polymer as the electrolyte. Coin cells were conditioned at 90 °C at a current density of 0.02 mA/cm² for 6 cycles to ensure stable SEI formation. Polarization was induced by applying a 40 mV potential for 1 hr. Impedance was measured before and after polarization, where a 20 mV bias was applied for the post polarization measurement. The impedance was then fit using EC-Lab software to extract resistance values used in the following equation used for calculating transference number:

$$t_{ss}^{+} = \frac{I_{ss}}{I_0} \left(\frac{\Delta V - I_0 R_0}{\Delta V - I_{ss} R_{ss}} \right)$$

3. RESULTS AND DISCUSSION

3.1. Molecular design and structural characterization of network electrolytes

Polymer networks were synthesized from PEO functionalized acrylate and diacrylate monomers, which were copolymerized with the trifluoromethane sulfonimide (TFSI) monomer (Figure 1), as confirmed by NMR (Figure 2). Acrylates were systematically investigated rather than methacrylates or styrenics because they have lower T_g due to the absence of α -methyl groups on the backbone or π - π interactions. The tethered anion of the ionic monomer makes this system a single cation conductor, while TFSI is bulky and charge delocalized, which weakens the electrostatic interactions with Li cations. A polar PEO chemistry further improves ion solvation and increases conductivity. A polar PEO chemistry further improves ion retworks, our acrylic EO monomers were synthesized to have precise lengths of crosslinker and comonomer rather than using commercially available EO diacrylates with a chain length distribution. By tuning the molar ratio between the crosslinker and comonomer, control of

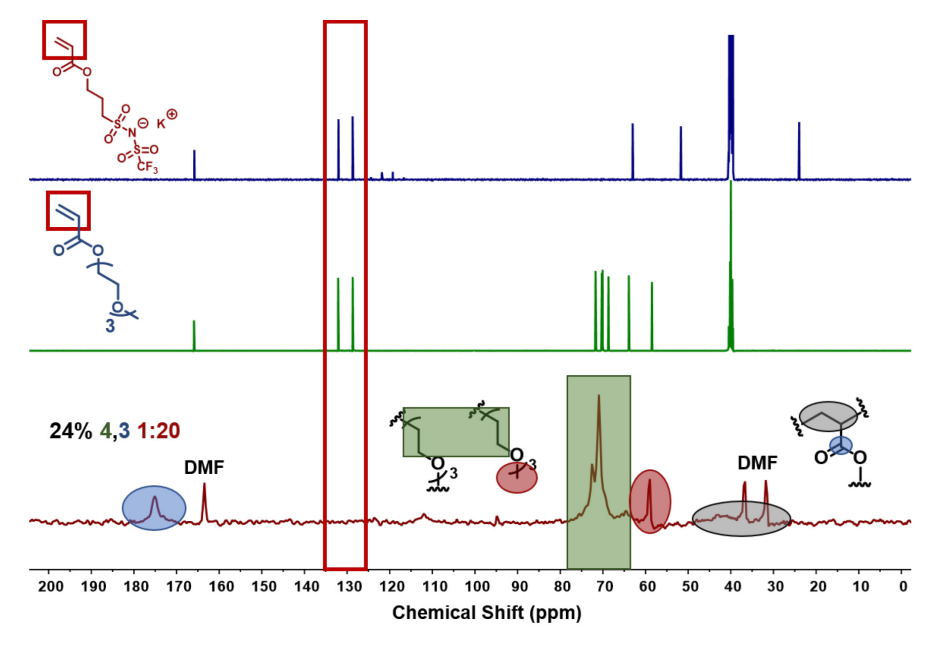


Figure 2. Solution phase ¹³C NMR of ionic monomer (top) and EO3 comonomer (middle) in DMSO-d₆. Solid state ¹³C NMR of 24% 4,3 1:20 network electrolyte (bottom) after curing shows the complete consumption of double bonds. The remaining peaks are in good agreement with the proposed network.

crosslinking density was achieved. The TFSI monomer content allows for systemically varying the ion concentration. The networks are named based on the mole percent of diacrylate crosslinker in the network (cl%), length of EO in the crosslinker (x), the length of EO on the comonomer (y), and the Li:EO ratio.

After the network was cured, Fourier-transform infrared spectroscopy (FTIR) and ¹³C solid state (SS) NMR were used to characterize the extent of the reaction. A complete disappearance of the C=C peaks at 127 and 133 ppm in ¹³C solid state NMR (Figure 2) compared to the monomers indicates that all of the vinyl groups have reacted within the resolution of this technique. Carbonyl peaks also shifted downfield from 165 ppm (monomers) to 173-177 ppm (final network) as the electron rich double bond adjacent to the C=O was reacted. Other peaks in the ¹³C NMR including 60-80 ppm (carbons in EO repeat units), and 35-45 ppm (methylene carbons in the backbone) agree with the proposed network structure. The consumption of acrylate monomer was also confirmed through the disappearance of terminal C=C bond stretches (900 cm⁻¹, and 1600-1700 **Table 1.** Summary of network electrolytes with varied mol% of crosslinker added (*cl%*), crosslinker

Table 1. Summary of network electrolytes with varied mol% of crosslinker added (cl%), crosslinker length (x), comonomer side chain (y), and Li:EO ratio. Average backbone atoms between junctions was calcuated based on the mol% of crosslinker and length of the crosslinker. Glass transition temperatures (T_g), 5% degradation temperature (T_d), conductivity at 90 °C and extent of ion exchange are also reported.

Entry	Sample	atoms between junctions	T _g (°C)	T _d (°C)	σ (at 90 °C) 10 ⁻⁶ S/cm	lon exchange extent
1	50% 4,3 1:20	9	17	309	0.68	96.3%
2	24% 4,3 1:20	11	-2	303	1.98	96.5%
3	24% 6,3 1:20	14	-9	303	3.8	94.6%
4	8% 6,3 1:20	22	-25	297	7.6	91.8%
5	24% 12,3 1:20	23	-19	304	9.1	90.7%
6	8% 12,3 1:20	31	-27	301	13.2	98.4%
7	4% 12,3 1:20	44	-29	298	14.1	90.8%
8	2% 12,3 1:20	69	-31	297	15.2	94.6%
9	1% 12,3 1:20	119	-33	295	13.3	95.1%
10	1% 12,3 1:30	119	-41	302	11.2	95.1%
11	1% 12,3 1:40	119	-45	304	9.7	95.5%
12	1% 12,3 1:50	119	-48	309	7.8	93.4%
13	1% 12,3 1:100	119	-53	312	3.2	95.8%
14	1% 12,6 1:30	119	-48	301	59.0	97.5%

cm⁻¹) in FTIR spectra of cured networks (Figure S2). After network formation, ion exchange was performed to replace K⁺ with Li⁺ using a 10-fold molar excess of LiClO₄. Control experiments compared the ionic conductivity and T_g of network samples after ion exchange durations of 24 and 48 hrs and showed no difference within error indicating an efficient exchange (Figure S3). The exchange was also quantified via mass spectroscopy by calculating the mole percent of Li⁺ relative to the total moles of Li⁺ and K⁺ (Table S1). In all cases, > 90% ion exchange extent was achieved as shown in Table 1. Each network was analyzed in terms of conductivity and Tg, with repeat measurements on independently prepared batches showing excellent agreement (Figure S4). A summary of all the network electrolytes is compiled in Table 1. The samples are named in terms of the 4 design variables: cl%, x, y, and Li:EO ratio. Because the crosslinkers have variable lengths, we have also calculated the average number of backbone atoms between crosslinks. All of the network electrolytes are transparent and self-standing as shown in Figure 1. As reported in Table 1, all the networks have good thermal stability ($T_d \sim 300$ °C) which is well above the temperatures used for processing and conductivity measurements. All samples were vacuum dried at 80 °C for 24 hrs and stored in an argon glovebox to minimize the effect of water.

3.2. Effect of polymer backbone

We first compared a methyl methacrylate (MMA) network with an otherwise identical methyl acrylate (MA) system using monomers shown in Figure 3a. The two 1% 12,3 1:30 networks were synthesized with the same procedure and as expected,⁷¹ the MMA network has a higher T_g of -16 °C compared to -41 °C for the MA electrolyte. As shown in Figure 3b, the MA electrolyte shows an order of magnitude higher ionic conductivity across the whole temperature range. After normalizing the conductivity to T_g, the data essentially overlap. Thus, we only pursued MA electrolytes for the remainder of this study.

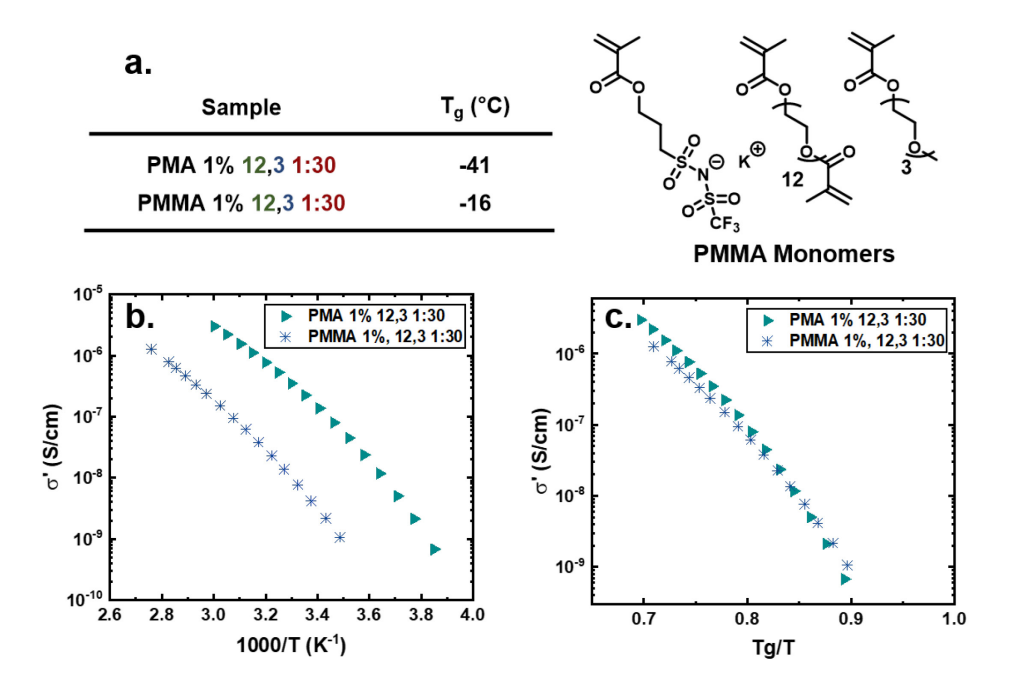


Figure 3. a) Glass transition temperatures of 1% 12,3 1:30 electrolytes with PMA and PMMA backbones. b) Ionic conductivity of the 1% 12,3 1:30 electrolytes on a raw and T_g -normalized scale reveal that the effect of backbone can be explained by the T_g difference.

3.3. Effect of crosslinker length (x) on conductivity

For networks with the shortest EO crosslinker (x = 4), entries 1-2 in Table 1, crosslinker are necessary to withstand swelling during ion exchange (Figure S5). Such network samples possess relatively high T_gs and the lowest ionic conductivities measured. Entries 3-6 contain EO crosslinkers (x = 6 or 12) and had 24 mol% or 8 mol% crosslinker, while the length of comonomer (y = 3) and Li:EO ratio (1:20) were held constant. Upon switching to longer crosslinkers (x = 6 or

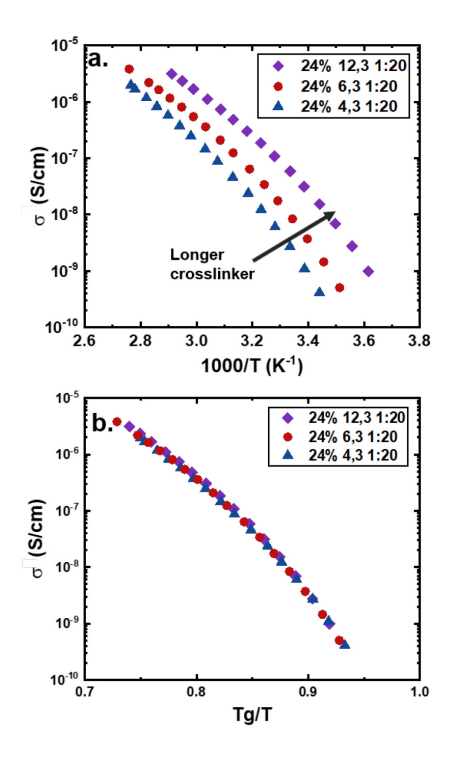


Figure 4. a) Ionic conductivity of samples with constant 24 mol% crosslinker, comonomer length y = 3, and Li:EO = 1:20 as a function of crosslinker length x. b) T_g -normalized conductivity reveals that the effect of x can be explained in terms of T_g shifts.

12), smooth and flexible networks were able to be synthesized at low crosslinker (< 8 mol%). As shown in Figure 4a, when the crosslinking is fixed at 24 mol% the conductivity systematically increases across the whole temperature range as x increases from 4 to 12. The change is as large as an order of magnitude, and this trend is directly related to the 17 °C decrease in T_g as shown in the T_g -normalized plot (Figure 4b) where the data overlaps. By increasing the length of the crosslinker from 4 to 12, the average backbone length between crosslinking junctions doubled resulting in a large drop in T_g . A similar trend is also observed in 8% crosslinking density electrolytes where a longer crosslinker shows higher conductivity due to lower T_g (Figure S6).

3.4. Effect of mol % of crosslinker (cl%) on conductivity and modulus

In entries 5-9 of Table 1, the variables x, y, Li:EO have been fixed to systematically investigate the role of crosslinker loading. For the 12,3 1:20 networks, the cl% was decreased from 24% to 1% corresponding to an increase in the average number of backbone atoms between crosslinks from 23 to 119. Although T_g systematically decreases (Table 1), the magnitude of decrease eventually plateaus. Conductivity increases significantly by lowering cl% from 24% to 8% (Figure 5a). We

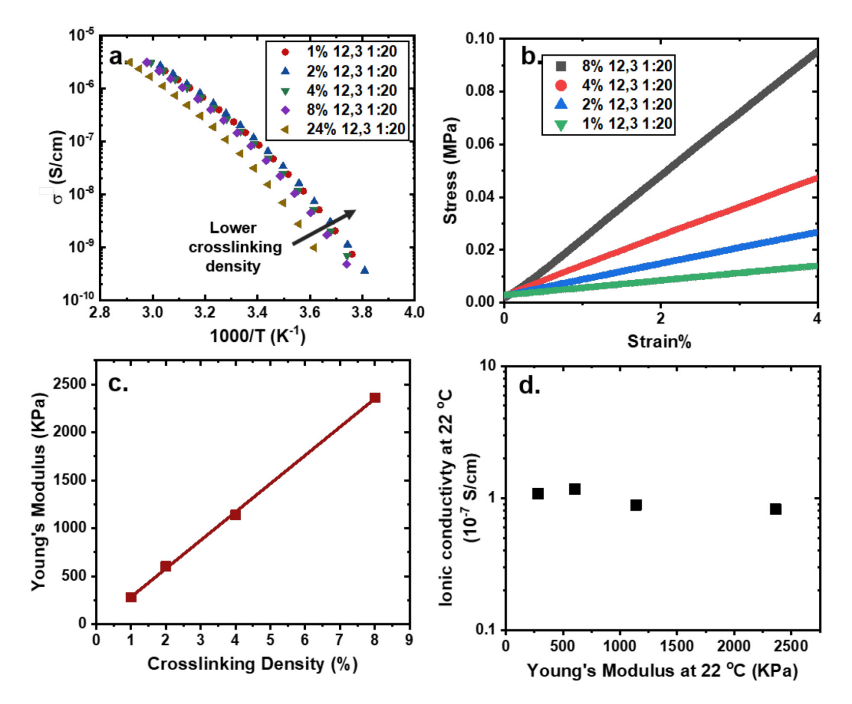


Figure 5. a) Ionic conductivity of cl% 12,3 1:20 network electrolytes only varying the crosslinking density as a function of temperature. b) Linear region of stress-strain curves measured on cl% 12,3 1:20 networks. c) Young's modulus of cl% 12,3 1:20 networks have a linear relationship with respect of crosslinking density. d) Ionic conductivity is invariant up to 8% crosslinking while modulus greatly increases.

note this is in qualitative agreement with prior work on PEO-polyurethane and PEO-acrylate networks with added LiTFSI salt where the ionic conductivity increased with decreasing crosslinker loadings.⁷²⁻⁷³ Similar trends have been observed in TFSI single anion conducting network systems.^{16, 74} At 8 mol% crosslinking and below, the conductivity is essentially invariant while a 24 mol% crosslinker sample begins to show a reduction. A normalized plot superposes the data as shown in Figure S7 indicating this is primarily a T_g effect. Figure 5b shows the linear region of the stress-strain curves of these networks which exhibits a linear relationship between

Young's modulus and crosslinking density as expected (Figure 5c). An important implication is that ionic conductivity only drops slightly for networks with 1 to 8 mol% crosslinker, yet the modulus increases by a factor of 8 (Figure 5d). In comparison with a linear block copolymer single ion conductor, conductivities are generally reported above 80 °C where the modulus is in the kPa range. The present crosslinked electrolytes can be as high as 2.4 MPa before impacting the conductivity. This provides a model system to deconvolute the roles of conductivity and modulus on electrolyte performance. This is also a useful design principle to improve the mechanical properties of network polymer electrolytes without impacting the ionic conductivity.

3.5. Effect of Li:EO ratio on conductivity

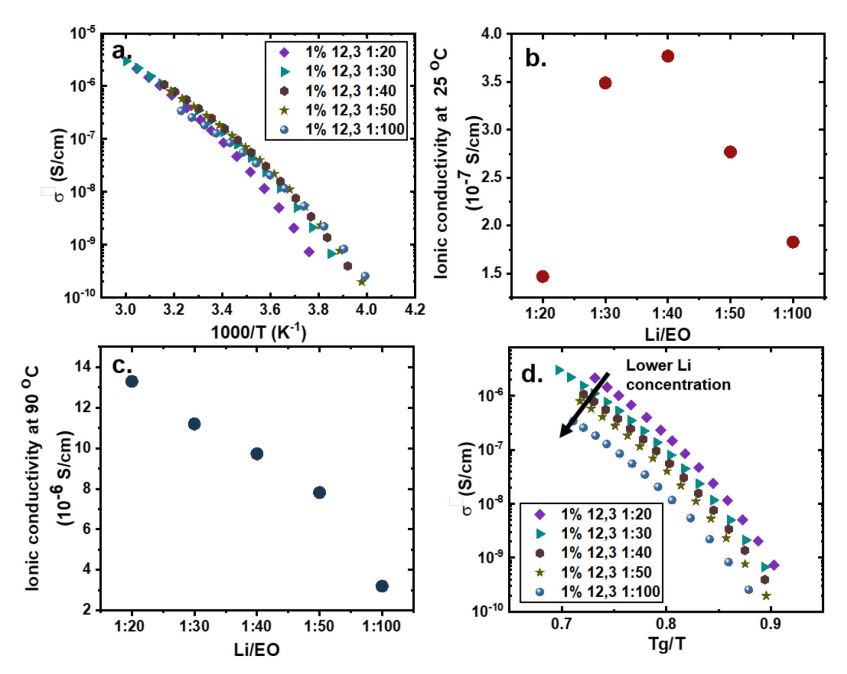


Figure 6. a) Ionic conductivity of network electrolyte 1% 12,3 Li:EO only varying the Li:EO ratio (1:20 to 1:100). b) Conductivity at room temperture is non-monotonic, while c) at high temperature increasing ionic content increases conductivity. d) Normalized conductivity of 1% 12,3 Li:EO networks reveals that T_g alone cannot superpose the data.

The role of the Li:EO ratio was investigated (entries 10-13 Table 1) with fixed cl%, x, and y networks. As shown in Figure 6a, a more complex conductivity trend is observed across a wide range of temperatures, despite the fact that T_g monotonically increases (from -53 to -33 °C) with

higher Li concentration (1:100 to 1:20 Table 1). At 25 °C a non-monotonic trend is observed with a maximum at 1:40 Li:EO ratio, similar to what has been observed in the literature with both PEO-salt systems^{30, 37, 69, 72, 75} and single ion conducting polymers.^{52-53, 76} This is attributed to a competition between ion concentration and ion mobility as segmental dynamics will be more important close to T_g. At high temperature (90 °C, Figure 6c), the conductivity monotonically decreases as total ion concentration decreases since all systems are at a temperature far above T_g where segmental dynamics plays a less important role. In a T_g-normalized plot (Figure 6d), conductivity decreases monotonically as the Li:EO ratio decreases from 1:20 to 1:100 across the entire temperature range. Such an observation is useful in designing electrolytes at different working temperature. At higher temperature, more ionic monomer will improve the conductivity whereas at lower temperature, fewer charges can lower T_g which ultimately improves conductivity.

3.6. Effect of comonomer length (y) and plasticizer

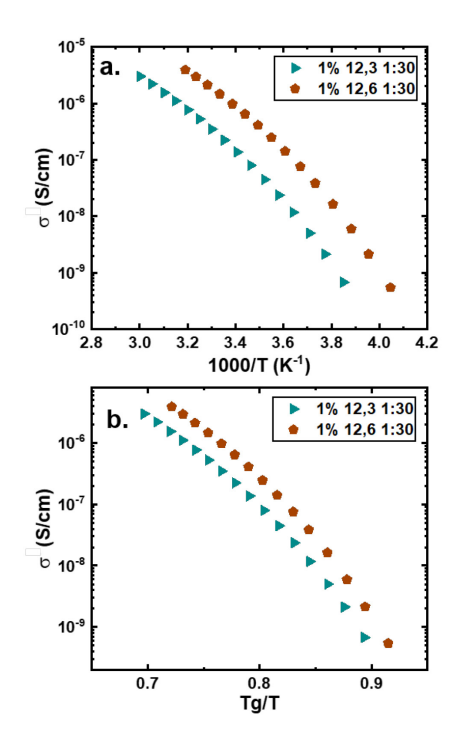


Figure 7. a) Ionic conductivity for fixed 1% 12, y 1:30 networks with two different comonomer lengths y. (b.) Normalized ionic conductivity shows that the enhancement is not simply a T_g effect and is attributed to improved ion solvation.

The final molecular variable we investigated was the role of comonomer length y for fixed cl%, x, Li:EO networks. An increase in ionic conductivity across the whole temperature range is observed (Figure 7a) as y increases from 3 to 6, accompanied by a 7 °C change in T_g . As shown in the T_g normalized ionic conductivity plot (Figure 7b), a significant increase in conductivity of the EO6 electrolyte persists suggesting that the T_g difference is not the main reason for the conductivity increase. For salt-in-polymer systems, a longer PEO side chain (6-7 EO repeat units) showed \sim 3 times higher ionic conductivity compared to the shorter (3 EO repeat units) side chain polymer. It is also known that the addition of 12-crown-4 ether into Li single ion conductor increases ionic conductivity due to better solvation provided by the crown structure. In our case, longer EO6 side chains provide a more stable coordination environment for Li⁺ solvation and

increase conductivity.⁷⁹

A conductivity on the order of 6×10^{-5} S/cm at high temperature is comparable to other reports of Li⁺ single ion conductors.^{33, 52-53, 76, 80-84} In many cases, small molecule organic solvent is added to boost the performance and form a gel electrolyte.^{29, 49, 80, 84} As shown in Figure S8, we have also measured ionic conductivity of the 1% 12,3 1:20 network electrolyte swollen with propylene carbonate (PC). At high temperature (90 °C) the ionic conductivity exceeds 10^{-4} S/cm and a preliminary transference number test indicates it is essentially a single ion conductor with t⁺ = 0.85 (Figure S11). Future work will investigate if such networks may be sufficient to suppress dendrites with and without solvent present.

4. CONCLUSION

In summary, a series of Li⁺ single ion conducting networks consisting of acrylate polymer backbone and EO side chains was designed and synthesized. By precisely controlling the molecular parameters, a detailed structure-property relationship of these network electrolytes was mapped out. It was shown at low crosslinking density (< 8 mol%), the modulus of the electrolyte can be increased by 8 times without sacrificing ionic conductivity, which can provide insights for the design of dendrite suppressing electrolytes. A maximum in the conductivity was observed at room temperature due to a competing effect of polymer dynamics and effective ion concentration, while far above T_g a monotonic increase of conductivity with respect to Li⁺ concentration was observed. Increasing the length of side chain from 3 to 6 EO units can also lead to a substantial increase in conductivity even after normalizing for T_g , and it is important to understand how relatively small changes in chemistry lead to such changes. In terms of our design variables cl%, x, y, and Li:EO, T_g can account for conductivity changes when x and cl% are varied. In contrast, T_g alone cannot account for changes in y and Li:EO. The best performing network electrolytes

studied have ionic conductivity on the order of 10^{-5} S/cm at high temperature which is comparable to other single ion conductors reported in the literature. Doping the network with 10 wt.% propylene carbonate increased this value to 10^{-4} S/cm.

ACKNOWLEDGMENTS

This work is funded by the Department of Materials Science and Engineering at the University of Illinois at Urbana Champaign (UIUC), the Energy Biosciences Institute through the EBI-Shell program (C. S., B. J.), and NSF DMR-1751291 (Q. Z.). We also acknowledge the use of facilities in the Materials Research Laboratory and School of Chemical Sciences at UIUC.

REFERENCE

- 1. Zu, C.-X.; Li, H., Thermodynamic analysis on energy densities of batteries. *Energy Environ. Sci.* **2011,** *4* (8), 2614-2624.
- 2. Mukhopadhyay, A.; Jangid, M. K., Li metal battery, heal thyself. Science 2018, 359 (6383), 1463.
- 3. Xu, W.; Wang, J.; Ding, F.; Chen, X.; Nasybulin, E.; Zhang, Y.; Zhang, J.-G., Lithium metal anodes for rechargeable batteries. *Energy Environ. Sci.* **2014,** *7* (2), 513-537.
- 4. Wood, K. N.; Kazyak, E.; Chadwick, A. F.; Chen, K. H.; Zhang, J. G.; Thornton, K.; Dasgupta, N. P., Dendrites and Pits: Untangling the Complex Behavior of Lithium Metal Anodes through Operando Video Microscopy. *ACS Cent Sci* **2016**, *2* (11), 790-801.
- 5. Aurbach, D.; Zinigrad, E.; Cohen, Y.; Teller, H., A short review of failure mechanisms of lithium metal and lithiatedgraphite anodes in liquid electrolyte solutions. *Solid State Ionics* **2002**, (148), 405-416.
- 6. Aurbach, D.; Daroux, M.; Faguy, P.; Yeager, E., Identification of surface films formed on lithium in propylene carbonate solutions. *J. Electrochem. Soc* **1987**, (134), 1611–1620.
- 7. Cheng, X.-B.; Zhang, R.; Zhao, C.-Z.; Zhang, Q., Toward safe lithium metal anode in rechargeable batteries: a review. *Chemical reviews* **2017**, *117* (15), 10403-10473.
- 8. Loveridge, M.; Remy, G.; Kourra, N.; Genieser, R.; Barai, A.; Lain, M.; Guo, Y.; Amor-Segan, M.; Williams, M.; Amietszajew, T.; Ellis, M.; Bhagat, R.; Greenwood, D., Looking Deeper into the Galaxy (Note 7). *Batteries* **2018**, *4* (1).
- 9. Sheridan, G. S.; Evans, C. M., Molecular Design of Precise Network Polymerized Ionic Liquid Membranes for Toluene/Heptane Separations. *Industrial & Engineering Chemistry Research* **2019**, *58* (31), 14389-14395.
- 10. Bara, J. E.; Hatakeyama, E. S.; Gabriel, C. J.; Zeng, X.; Lessmann, S.; Gin, D. L.; Noble, R. D., Synthesis and light gas separations in cross-linked gemini room temperature ionic liquid polymer membranes. *Journal of Membrane Science* **2008**, *316* (1-2), 186-191.
- 11. Tomé, L. C.; Mecerreyes, D.; Freire, C. S.; Rebelo, L. P. N.; Marrucho, I. M., Pyrrolidinium-based polymeric ionic liquid materials: New perspectives for CO2 separation membranes. *Journal of membrane science* **2013**, *428*, 260-266.

- 12. Izák, P.; Ruth, W.; Fei, Z.; Dyson, P. J.; Kragl, U., Selective removal of acetone and butan-1-ol from water with supported ionic liquid–polydimethylsiloxane membrane by pervaporation. *Chemical Engineering Journal* **2008**, *139* (2), 318-321.
- 13. Gu, Y.; Lodge, T. P., Synthesis and gas separation performance of triblock copolymer ion gels with a polymerized ionic liquid mid-block. *Macromolecules* **2011**, *44* (7), 1732-1736.
- 14. Bara, J. E.; Lessmann, S.; Gabriel, C. J.; Hatakeyama, E. S.; Noble, R. D.; Gin, D. L., Synthesis and performance of polymerizable room-temperature ionic liquids as gas separation membranes. *Industrial & engineering chemistry research* **2007**, *46* (16), 5397-5404.
- 15. Carlisle, T. K.; Wiesenauer, E. F.; Nicodemus, G. D.; Gin, D. L.; Noble, R. D., Ideal CO2/light gas separation performance of poly (vinylimidazolium) membranes and poly (vinylimidazolium)-ionic liquid composite films. *Industrial & Engineering Chemistry Research* **2013**, *52* (3), 1023-1032.
- 16. Shen, C.; Zhao, Q.; Evans, C. M., Precise Network Polymerized Ionic Liquids for Low-Voltage, Dopant-Free Soft Actuators. *Advanced Materials Technologies* **2019**, *4* (2), 1800535.
- 17. Lu, J.; Kim, S. G.; Lee, S.; Oh, I. K., A Biomimetic Actuator Based on an Ionic Networking Membrane of Poly (styrene-alt-maleimide)-Incorporated Poly (vinylidene fluoride). *Advanced Functional Materials* **2008**, *18* (8), 1290-1298.
- 18. Kokubo, H.; Sano, R.; Murai, K.; Ishii, S.; Watanabe, M., Ionic polymer actuators using poly (ionic liquid) electrolytes. *European Polymer Journal* **2018**, *106*, 266-272.
- 19. Yan, Y.; Santaniello, T.; Bettini, L. G.; Minnai, C.; Bellacicca, A.; Porotti, R.; Denti, I.; Faraone, G.; Merlini, M.; Lenardi, C., Electroactive ionic soft actuators with monolithically integrated gold nanocomposite electrodes. *Advanced Materials* **2017**, *29* (23), 1606109.
- 20. Kim, O.; Shin, T. J.; Park, M. J., Fast low-voltage electroactive actuators using nanostructured polymer electrolytes. *Nature communications* **2013**, *4*, 2208.
- 21. Dang, H.-S.; Jannasch, P., A comparative study of anion-exchange membranes tethered with different hetero-cycloaliphatic quaternary ammonium hydroxides. *Journal of Materials Chemistry A* **2017,** *5* (41), 21965-21978.
- 22. You, W.; Padgett, E.; MacMillan, S. N.; Muller, D. A.; Coates, G. W., Highly conductive and chemically stable alkaline anion exchange membranes via ROMP of trans-cyclooctene derivatives. *Proceedings of the National Academy of Sciences* **2019**, *116* (20), 9729-9734.
- 23. Zhu, L.; Yu, X.; Peng, X.; Zimudzi, T. J.; Saikia, N.; Kwasny, M. T.; Song, S.; Kushner, D. I.; Fu, Z.; Tew, G. N., Poly (olefin)-Based Anion Exchange Membranes Prepared Using Ziegler–Natta Polymerization. *Macromolecules* **2019**.
- 24. Zhu, L.; Peng, X.; Shang, S. L.; Kwasny, M. T.; Zimudzi, T. J.; Yu, X.; Saikia, N.; Pan, J.; Liu, Z. K.; Tew, G. N., High Performance Anion Exchange Membrane Fuel Cells Enabled by Fluoropoly (olefin) Membranes. *Advanced Functional Materials* **2019**, 1902059.
- 25. Jeon, J. Y.; Park, S.; Han, J.; Maurya, S.; Mohanty, A. D.; Tian, D.; Saikia, N.; Hickner, M. A.; Ryu, C. Y.; Tuckerman, M. E., Synthesis of Aromatic Anion Exchange Membranes by Friedel–Crafts Bromoalkylation and Cross-Linking of Polystyrene Block Copolymers. *Macromolecules* **2019**, *52* (5), 2139-2147.
- 26. Ford, H. O.; Merrill, L. C.; He, P.; Upadhyay, S. P.; Schaefer, J. L., Cross-Linked Ionomer Gel Separators for Polysulfide Shuttle Mitigation in Magnesium–Sulfur Batteries: Elucidation of Structure–Property Relationships. *Macromolecules* **2018**, *51* (21), 8629-8636.
- 27. Tatsuma, T.; Taguchi, M.; Oyama, N., Inhibition effect of covalently cross-linked gel electrolytes on lithium dendrite formation. *Electrochimica acta* **2001**, *46* (8), 1201-1205.
- 28. Khurana, R.; Schaefer, J. L.; Archer, L. A.; Coates, G. W., Suppression of lithium dendrite growth using cross-linked polyethylene/poly (ethylene oxide) electrolytes: a new approach for practical lithium-metal polymer batteries. *Journal of the American Chemical Society* **2014**, *136* (20), 7395-7402.

- 29. Baik, J.-H.; Kim, S.; Hong, D. G.; Lee, J.-C., Gel Polymer Electrolytes Based on Polymerizable Lithium Salt and Poly (ethylene glycol) for Lithium Battery Applications. *ACS applied materials & interfaces* **2019**.
- 30. Nishimoto, A.; Agehara, K.; Furuya, N.; Watanabe, T.; Watanabe, M., High ionic conductivity of polyether-based network polymer electrolytes with hyperbranched side chains. *Macromolecules* **1999**, *32* (5), 1541-1548.
- 31. Tong, Y.; Lyu, H.; Xu, Y.; Thapaliya, B. P.; Li, P.; Sun, X.-G.; Dai, S., All-solid-state interpenetrating network polymer electrolytes for long cycle life of lithium metal batteries. *Journal of Materials Chemistry A* **2018**, *6* (30), 14847-14855.
- 32. Chopade, S. A.; Au, J. G.; Li, Z.; Schmidt, P. W.; Hillmyer, M. A.; Lodge, T. P., Robust polymer electrolyte membranes with high ambient-temperature lithium-ion conductivity via polymerization-induced microphase separation. *ACS applied materials & interfaces* **2017**, *9* (17), 14561-14565.
- 33. Sun, X.-G.; Reeder, C. L.; Kerr, J. B., Synthesis and characterization of network type single ion conductors. *Macromolecules* **2004**, *37* (6), 2219-2227.
- 34. Driscoll, P. F.; Yang, L.; Gervais, M.; Kerr, J. B., Polyelectrolyte Membranes Containing Lithium Malonato (difluoro) borate for Lithium-Ion Systems. *ECS Transactions* **2011**, *33* (23), 33-53.
- 35. Zhao, Q.; Shen, C.; Halloran, K. P.; Evans, C. M., Effect of Network Architecture and Linker Polarity on Ion Aggregation and Conductivity in Precise Polymerized Ionic Liquids. *ACS Macro Letters* **2019**, *8*, 658-663.
- 36. Kono, M.; Hayashi, E.; Watanabe, M., Network polymer electrolytes with free chain ends as internal plasticizer. *Journal of the Electrochemical Society* **1998**, *145* (5), 1521-1527.
- 37. Watanabe, M.; Nishimoto, A., Effects of network structures and incorporated salt species on electrochemical properties of polyether-based polymer electrolytes. *Solid State Ionics* **1995**, *79*, 306-312.
- 38. Watanabe, M.; Nagano, S.; Sanui, K.; Ogata, N., Ionic conductivity of network polymers from poly (ethylene oxide) containing lithium perchlorate. *Polymer journal* **1986**, *18* (11), 809.
- 39. Tatsuma, T.; Taguchi, M.; Iwaku, M.; Sotomura, T.; Oyama, N., Inhibition effects of polyacrylonitrile gel electrolytes on lithium dendrite formation. *Journal of Electroanalytical Chemistry* **1999**, *472* (2), 142-146.
- 40. Lu, Q.; He, Y. B.; Yu, Q.; Li, B.; Kaneti, Y. V.; Yao, Y.; Kang, F.; Yang, Q. H., Dendrite-Free, High-Rate, Long-Life Lithium Metal Batteries with a 3D Cross-Linked Network Polymer Electrolyte. *Advanced Materials* **2017**, *29* (13), 1604460.
- 41. Laik, B.; Legrand, L.; Chausse, A.; Messina, R., Ion—ion interactions and lithium stability in a crosslinked PEO containing lithium salts. *Electrochimica acta* **1998**, *44* (5), 773-780.
- 42. Zheng, Q.; Ma, L.; Khurana, R.; Archer, L. A.; Coates, G. W., Structure—property study of cross-linked hydrocarbon/poly (ethylene oxide) electrolytes with superior conductivity and dendrite resistance. *Chemical Science* **2016**, *7* (11), 6832-6838.
- 43. Jing, B. B.; Evans, C. M., Catalyst-Free Dynamic Networks for Recyclable, Self-Healing Solid Polymer Electrolytes. *Journal of the American Chemical Society* **2019**, *141* (48), 18932-18937.
- 44. Zugmann, S.; Fleischmann, M.; Amereller, M.; Gschwind, R. M.; Wiemhöfer, H. D.; Gores, H. J., Measurement of transference numbers for lithium ion electrolytes via four different methods, a comparative study. *Electrochimica Acta* **2011**, *56* (11), 3926-3933.
- 45. Zhang, Z.; Wheatle, B. K.; Krajniak, J.; Keith, J. R.; Ganesan, V., Ion Mobilities, Transference Numbers, and Inverse Haven Ratios of Polymeric Ionic Liquids. *ACS Macro Letters* **2019**, *9*, 84-89.
- 46. Shah, D. B.; Nguyen, H. Q.; Grundy, L. S.; Olson, K. R.; Mecham, S. J.; DeSimone, J. M.; Balsara, N. P., Difference between approximate and rigorously measured transference numbers in fluorinated electrolytes. *Physical Chemistry Chemical Physics* **2019**, *21* (15), 7857-7866.

- 47. Fong, K. D.; Self, J.; Diederichsen, K. M.; Wood, B. M.; McCloskey, B. D.; Persson, K. A., Ion Transport and the True Transference Number in Nonaqueous Polyelectrolyte Solutions for Lithium Ion Batteries. *ACS central science* **2019**, *5* (7), 1250-1260.
- 48. Monroe, C.; Newman, J., Dendrite growth in lithium/polymer systems a propagation model for liquid electrolytes under galvanostatic conditions. *Journal of The Electrochemical Society* **2003**, *150* (10), A1377-A1384.
- 49. Luo, G.; Yuan, B.; Guan, T.; Cheng, F.; Zhang, W.; Chen, J., Synthesis of Single Lithium-Ion Conducting Polymer Electrolyte Membrane for Solid-State Lithium Metal Batteries. *ACS Applied Energy Materials* **2019**.
- 50. Porcarelli, L.; Shaplov, A. S.; Bella, F.; Nair, J. R.; Mecerreyes, D.; Gerbaldi, C., Single-ion conducting polymer electrolytes for lithium metal polymer batteries that operate at ambient temperature. *ACS Energy Letters* **2016**, *1* (4), 678-682.
- 51. Lu, Y.; Tikekar, M.; Mohanty, R.; Hendrickson, K.; Ma, L.; Archer, L. A., Stable cycling of lithium metal batteries using high transference number electrolytes. *Advanced Energy Materials* **2015**, *5* (9), 1402073.
- 52. Devaux, D.; Liénafa, L.; Beaudoin, E.; Maria, S.; Phan, T. N.; Gigmes, D.; Giroud, E.; Davidson, P.; Bouchet, R., Comparison of single-ion-conductor block-copolymer electrolytes with Polystyrene-TFSI and Polymethacrylate-TFSI structural blocks. *Electrochimica Acta* **2018**, *269*, 250-261.
- 53. Bouchet, R.; Maria, S.; Meziane, R.; Aboulaich, A.; Lienafa, L.; Bonnet, J.-P.; Phan, T. N.; Bertin, D.; Gigmes, D.; Devaux, D., Single-ion BAB triblock copolymers as highly efficient electrolytes for lithium-metal batteries. *Nature materials* **2013**, *12* (5), 452.
- 54. Rojas, A. A.; Thakker, K.; McEntush, K. D.; Inceoglu, S.; Stone, G. M.; Balsara, N. P., Dependence of Morphology, Shear Modulus, and Conductivity on the Composition of Lithiated and Magnesiated Single-Ion-Conducting Block Copolymer Electrolytes. *Macromolecules* **2017**, *50* (21), 8765-8776.
- 55. Elmore, C. T.; Seidler, M. E.; Ford, H. O.; Merrill, L. C.; Upadhyay, S. P.; Schneider, W. F.; Schaefer, J. L., Ion transport in solvent-free, crosslinked, single-ion conducting polymer electrolytes for post-lithium ion batteries. *Batteries* **2018**, *4* (2), 28.
- 56. Singh, M.; Odusanya, O.; Wilmes, G. M.; Eitouni, H. B.; Gomez, E. D.; Patel, A. J.; Chen, V. L.; Park, M. J.; Fragouli, P.; latrou, H., Effect of molecular weight on the mechanical and electrical properties of block copolymer electrolytes. *Macromolecules* **2007**, *40* (13), 4578-4585.
- 57. Mecerreyes, D., Polymeric ionic liquids: Broadening the properties and applications of polyelectrolytes. *Progress in Polymer Science* **2011**, *36* (12), 1629-1648.
- 58. Choi, U. H.; Ye, Y.; Salas de la Cruz, D.; Liu, W.; Winey, K. I.; Elabd, Y. A.; Runt, J.; Colby, R. H., Dielectric and viscoelastic responses of imidazolium-based ionomers with different counterions and side chain lengths. *Macromolecules* **2014**, *47* (2), 777-790.
- 59. Yuan, J.; Mecerreyes, D.; Antonietti, M., Poly (ionic liquid) s: An update. *Progress in Polymer Science* **2013**, *38* (7), 1009-1036.
- 60. Inceoglu, S.; Rojas, A. A.; Devaux, D.; Chen, X. C.; Stone, G. M.; Balsara, N. P., Morphology–conductivity relationship of single-ion-conducting block copolymer electrolytes for lithium batteries. *ACS Macro Letters* **2014**, *3* (6), 510-514.
- 61. Shen, C.; Zhao, Q.; Evans, C. M., Ion specific, odd—even glass transition temperatures and conductivities in precise network polymerized ionic liquids. *Molecular Systems Design & Engineering* **2019**, *4* (2), 332-341.
- Rhoades, T. C.; Wistrom, J. C.; Johnson, R. D.; Miller, K. M., Thermal, mechanical and conductive properties of imidazolium-containing thiol-ene poly (ionic liquid) networks. *Polymer* **2016**, *100*, 1-9.
- 63. Nguyen, A.; Rhoades, T. C.; Johnson, R. D.; Miller, K. M., Influence of Anion and Crosslink Density on the Ionic Conductivity of 1, 2, 3-Triazolium-Based Poly (ionic liquid) Polyester Networks. *Macromolecular Chemistry and Physics* **2017**, *218* (21), 1700337.

- 64. Tracy, C. A.; Adler, A. M.; Nguyen, A.; Johnson, R. D.; Miller, K. M., Covalently crosslinked 1, 2, 3-triazolium-containing polyester networks: thermal, mechanical, and conductive properties. *ACS omega* **2018**, *3* (10), 13442-13453.
- 65. Phan, T. N.; Ferrand, A.; Liénafa, L.; Rollet, M.; Maria, S.; Bouchet, R.; Gigmes, D., Vinyl monomers bearing a sulfonyl (trifluoromethane sulfonyl) imide group: synthesis and polymerization using nitroxide-mediated polymerization. *Polymer Chemistry* **2016**, *7* (45), 6901-6910.
- 66. https://polymerdatabase.com/polymer%20physics/Polymer%20Tg.html Polymer Properties Database.
- 67. Aravindan, V.; Gnanaraj, J.; Madhavi, S.; Liu, H. K., Lithium-ion conducting electrolyte salts for lithium batteries. *Chemistry–A European Journal* **2011**, *17* (51), 14326-14346.
- 68. Seo, D. M.; Borodin, O.; Han, S.-D.; Boyle, P. D.; Henderson, W. A., Electrolyte solvation and ionic association II. Acetonitrile-lithium salt mixtures: highly dissociated salts. *Journal of The Electrochemical Society* **2012**, *159* (9), A1489-A1500.
- 69. Xue, Z.; He, D.; Xie, X., Poly (ethylene oxide)-based electrolytes for lithium-ion batteries. *Journal of Materials Chemistry A* **2015**, *3* (38), 19218-19253.
- 70. Prasanth, R.; Shubha, N.; Hng, H. H.; Srinivasan, M., Effect of poly (ethylene oxide) on ionic conductivity and electrochemical properties of poly (vinylidenefluoride) based polymer gel electrolytes prepared by electrospinning for lithium ion batteries. *Journal of Power Sources* **2014**, *245*, 283-291.
- 71. Krause, S.; Gormley, J. J.; Roman, N.; Shetter, J. A.; Watanabe, W. H., Glass temperatures of some acrylic polymers. *Journal of Polymer Science Part A: General Papers* **1965**, *3* (10), 3573-3586.
- 72. Carvalho, L.; Guégan, P.; Cheradame, H.; Gomes, A., Variation of the mesh size of PEO-based networks filled with TFSILi: from an Arrhenius to WLF type conductivity behavior. *European polymer journal* **2000**, *36* (2), 401-409.
- 73. D'Angelo, A. J.; Panzer, M. J., Enhanced Lithium Ion Transport in Poly (ethylene glycol) Diacrylate-Supported Solvate Ionogel Electrolytes via Chemically Cross-linked Ethylene Oxide Pathways. *The Journal of Physical Chemistry B* **2017**, *121* (4), 890-895.
- 74. Washiro, S.; Yoshizawa, M.; Nakajima, H.; Ohno, H., Highly ion conductive flexible films composed of network polymers based on polymerizable ionic liquids. *Polymer* **2004**, *45* (5), 1577-1582.
- 75. Lascaud, S.; Perrier, M.; Vallee, A.; Besner, S.; Prud'Homme, J.; Armand, M., Phase diagrams and conductivity behavior of poly (ethylene oxide)-molten salt rubbery electrolytes. *Macromolecules* **1994**, *27* (25), 7469-7477.
- 76. Feng, S.; Shi, D.; Liu, F.; Zheng, L.; Nie, J.; Feng, W.; Huang, X.; Armand, M.; Zhou, Z., Single lithium-ion conducting polymer electrolytes based on poly [(4-
- styrenesulfonyl)(trifluoromethanesulfonyl) imide] anions. Electrochimica Acta 2013, 93, 254-263.
- 77. Cowie, J.; Sadaghianizadeh, K., Effect of side chain length and crosslinking on the ac conductivity of oligo (ethyleneoxide) comb-branch polymer-salt mixtures. *Solid State Ionics* **1990**, *42* (3-4), 243-249.
- 78. Choi, U. H.; Colby, R. H., The Role of Solvating 12-Crown-4 Plasticizer on Dielectric Constant and Ion Conduction of Poly (ethylene oxide) Single-Ion Conductors. *Macromolecules* **2017**, *50* (14), 5582-5591.
- 79. Miller III, T. F.; Wang, Z.-G.; Coates, G. W.; Balsara, N. P., Designing polymer electrolytes for safe and high capacity rechargeable lithium batteries. *Accounts of chemical research* **2017**, *50* (3), 590-593.
- 80. Park, C. H.; Sun, Y.-K.; Kim, D.-W., Blended polymer electrolytes based on poly (lithium 4-styrene sulfonate) for the rechargeable lithium polymer batteries. *Electrochimica acta* **2004**, *50* (2-3), 375-378.
- 81. Sun, X.-G.; Hou, J.; Kerr, J. B., Comb-shaped single ion conductors based on polyacrylate ethers and lithium alkyl sulfonate. *Electrochimica acta* **2005**, *50* (5), 1139-1147.
- 82. Ma, Q.; Zhang, H.; Zhou, C.; Zheng, L.; Cheng, P.; Nie, J.; Feng, W.; Hu, Y. S.; Li, H.; Huang, X., Single lithium-ion conducting polymer electrolytes based on a super-delocalized polyanion. *Angewandte Chemie International Edition* **2016**, *55* (7), 2521-2525.

- 83. Porcarelli, L.; Shaplov, A. S.; Salsamendi, M.; Nair, J. R.; Vygodskii, Y. S.; Mecerreyes, D.; Gerbaldi, C., Single-ion block copoly (ionic liquid) s as electrolytes for all-solid state lithium batteries. *ACS applied materials & interfaces* **2016**, *8* (16), 10350-10359.
- 84. Jeong, K.; Park, S.; Lee, S.-Y., Revisiting polymeric single lithium-ion conductors as an organic route for all-solid-state lithium ion and metal batteries. *Journal of materials chemistry A* **2019**, *7* (5), 1917-1935.

SUPPORTING INFORMATION

Detailed characterization data of monomers and Li⁺ conducting polymer network is documented in the Supporting Information.

TOC graphic

